

Symmetry Constraints on Pion Valence Structure

Xiaobin Wang (王晓斌)^{ID,1}, Lei Chang (常雷)^{ID,1},
Minghui Ding (丁明慧)^{ID,2,3}, Khépani Raya^{ID,4} and Craig D. Roberts^{ID,2,5}

¹*School of Physics, Nankai University, Tianjin 300071, China*

²*School of Physics, Nanjing University, Nanjing, Jiangsu 210093, China*

³*Institute for Nonperturbative Physics, Nanjing University, Nanjing, Jiangsu 210093, China*

⁴*Department of Integrated Sciences and Center for Advanced Studies in Physics,
Mathematics and Computation, University of Huelva, E-21071 Huelva, Spain.*

⁵*Institute for Nonperturbative Physics, Nanjing University, Nanjing, Jiangsu 210093, China*
Email: leichang@nankai.edu.cn (LC); mhding@nju.edu.cn (MD); cdroberts@nju.edu.cn (CDR)

(Dated: 2025 October 26)

The profile of the pion valence quark distribution function (DF) remains controversial. Working from the concepts of QCD effective charges and generalised parton distributions, we show that since the pion elastic electromagnetic form factor is well approximated by a monopole, then, at large light-front momentum fraction, the pion valence quark DF is a convex function described by a large- x power law that is practically consistent with expectations based on quantum chromodynamics.

1. Introduction—Pions are the messengers of Nature’s strong interaction, being responsible for the long-range binding that stabilises all nuclei. There are three pions: π^\pm, π^0 . They form an isospin triplet. The π^\pm are a both particle antiparticle pairs; hence, they are mass degenerate. The π^0 is its own antiparticle and is almost mass degenerate with π^\pm . The small splitting, $[m_{\pi^\pm} - m_{\pi^0}]/m_{\pi^\pm} = 3.3\%$ [1], owes to isospin-symmetry breaking in the strong interaction, which is small, and electromagnetic contributions.

In effective theories of nuclear interactions, pions are typically considered to be point particles [2–4]. However, they are not. Pions exhibit a special dichotomy. Supposing that quantum chromodynamics (QCD) is the theory underlying strong interactions [5], then pions are both [6–10]: (a) the Goldstone bosons that emerge as a consequence of dynamical chiral symmetry breaking in QCD and (b) QCD bound states, seeded by a light valence quark (u – up; d – down) and a light valence antiquark.

Pion structure was first explored in experiments that determined the π^\pm charge radius [11–13]: its radius is roughly 80% of that of the proton [1], so the pion is far from pointlike. Interior structural information has been obtained using $\pi + W$ Drell-Yan reactions [14, 15, E615] and deep-inelastic scattering (DIS) reactions $ep \rightarrow e'\pi^+n$, *i.e.*, DIS on a proton target with a tagged neutron in the final state [16, 17].

Only the E615 data provide information on pion valence quark structure and analyses of that data continue to be controversial [18–26]. The data are intended to inform our understanding of the valence quark distribution function (DF), $L_\pi(x; \zeta)$, which is a nonnegative density that describes the probability that a given valence quark carries a light-front fraction of the pion’s momentum in the range $[x + dx, x]$ when perceived by a probe with resolving energy scale ζ . Herein, we deliver a collection of model-independent and parameter-free predictions that constrain the behaviour of the pion valence quark DF.

2. Hadron scale and DF symmetries—We begin with

the concept of a QCD effective charge [27, 28]. In this scheme, a QCD running coupling is defined using the expansion of a chosen observable restricted to first order in the perturbative coupling, α_s ; see the discussion in Ref. [29, Sec. 4.3]. Consequently, effective charges are typically process dependent, like $\alpha_{g_1}(k^2)$, defined via the Bjorken sum rule [30]. Significantly, any coupling obtained in this way is analogous to the Gell-Mann–Low coupling in quantum electrodynamics [31]. Moreover, it is: consistent with the QCD renormalisation group; renormalisation scheme independent; everywhere analytic and finite; and supplies an infrared completion of any standard (perturbatively defined) running coupling.

Herein, we elect to work with an effective charge, $\alpha_{1\ell}(k^2)$, that is a function which, when used to integrate the leading-order perturbative DGLAP equations [32–35], defines an evolution scheme for all parton DFs – both unpolarised and polarised, and for any hadron – that is all-orders exact. This is the all-orders (AO) approach [36]. The definition is broader than usual because it refers to an entire class of observables, not just a single measurable quantity. It is important to stress that the pointwise form $\alpha_{1\ell}(k^2)$ is largely irrelevant: a large array of model-independent results can be proved without any reference to the k^2 -profile of the effective charge [36].

Suppose now that one has a π^+ valence quark DF at some scale $\zeta \gg m_p$, where m_p is the proton mass, *i.e.*, $u_\pi(x, \zeta)$, where $x \in [0, 1]$. Owing to \mathcal{G} -parity symmetry [37], which is a good approximation in Nature, then [38]:

$$u_{\pi^+}(x, \zeta) = \bar{d}_{\pi^+}(x; \zeta), \quad (1)$$

with similar statements for $\pi^{-,0}$.

Given the existence of $\alpha_{1\ell}(k^2)$, which is available at all k^2 , by definition, a next step is possible. Namely, one can use $\alpha_{1\ell}(k^2)$ -extended DGLAP evolution, *viz.* the AO method, to evolve $u_{\pi^+}(x, \zeta)$ to a scale $\zeta_{\mathcal{H}} \lesssim m_p$, whereat all properties of the pion – including its light-front momentum – are carried by its valence degrees of freedom. This is the hadron scale, $\zeta_{\mathcal{H}}$. The numerical value of $\zeta_{\mathcal{H}}$

is immaterial. One need only know that it exists; a fact guaranteed by the theory of effective charges.

At $\zeta_{\mathcal{H}}$, the valence-quark and -antiquark are quasiparticles, into which all glue and sea partons have been sublimated [39]. This is just a statement of dressing and is expressed analogously in any QCD Schwinger function; consider, *e.g.*, a diagrammatic expansion of the quark gap equation. Exploiting Eq. (1), it follows that

$$u_{\pi^+}(x, \zeta_{\mathcal{H}}) = \bar{d}_{\pi^+}(x) = u_{\pi^+}(1-x, \zeta_{\mathcal{H}}), \quad (2)$$

because symmetry requires that the light-front momentum be shared equally between the valence constituents. Thus, at the hadron scale, there is only one nontrivial DF, which is that of the valence u quark in the π^+ .

As explained elsewhere [36], these statements are true by definition. The issue is whether anything useful can therefrom be said about hadron observables. Today, one can answer in the affirmative because this approach has proved efficacious in many applications, providing, *e.g.*, unified predictions for all – including glue and sea – pion and kaon DFs [40]; all proton, Λ , Σ^0 DFs [41–45]; insights from experiment into such DFs [46, 47]; useful information on quark and gluon angular momentum contributions to the proton spin [48]; predictions for π and K fragmentation functions [49]; and a tenable species separation of nucleon gravitational form factors [50, 51].

Using the overlap representation of generalised parton distributions (GPDs) [52], one has the following expression for the pion valence quark GPD:

$$H^{u\pi}(x, Q^2; \zeta_{\mathcal{H}}) = \int d^2 b_{\perp} e^{i(1-x)b_{\perp} \cdot Q} |\psi^{u\pi}(x, b_{\perp}; \zeta_{\mathcal{H}})|^2, \quad (3)$$

where $\psi^{u\pi}(x, b_{\perp}; \zeta_{\mathcal{H}})$ is the pion valence-quark light-front wave function in impact parameter space [53]: b_{\perp} is Fourier conjugate to k_{\perp} , the hadron momentum in the light-front transverse plane. (Herein, we need only consider zero skewness.) Canonical normalisation requires

$$\int_0^1 dx \int d^2 b_{\perp} |\psi^{u\pi}(x, b_{\perp}; \zeta_{\mathcal{H}})|^2 = 1. \quad (4)$$

Furthermore and importantly [54]:

$$u_{\pi}(x, \zeta_{\mathcal{H}}) = H^{u\pi}(x, Q^2 = 0; \zeta_{\mathcal{H}}), \quad (5)$$

i.e., the pion valence quark DF is the $Q^2 = 0$ (forward) limit of the pion valence quark GPD. Such DFs are non-negative functions.

In the AO evolution setting, there is no other component of $\psi^{u\pi}(x, b_{\perp}; \zeta_{\mathcal{H}})$ at $\zeta_{\mathcal{H}}$. Thus, symmetry entails

$$\psi^{u\pi}(x, b_{\perp}; \zeta_{\mathcal{H}}) = \psi^{u\pi}(1-x, b_{\perp}; \zeta_{\mathcal{H}}); \quad (6)$$

hence, using Eq. (3),

$$H^{u\pi}(x, Q^2; \zeta_{\mathcal{H}}) = H^{u\pi}(1-x, Q^2[1-x]^2/x^2; \zeta_{\mathcal{H}}). \quad (7)$$

Thus far, only \mathcal{G} -parity symmetry has been used.

3. Constraints via pion electromagnetic form factor — The pion form factor, $F_{\pi}(Q^2)$, has been measured [11–13, 55, 56]. Existing data, available on $0 < Q^2/\text{GeV}^2 \leq 2.45$, are well approximated by the following monopole function [57]:

$$F_{\pi}^M(Q^2) = 1/(1 + Q^2/m_M^2), \quad m_M \approx 0.73 \text{ GeV}. \quad (8)$$

On the other hand, perturbative QCD (pQCD) predicts [58–60] that on some domain $Q^2 \gg m_p^2$, $F_{\pi}(Q^2)$ falls faster than a monopole, with the additional logarithmic suppression expressing the impact of anomalous dimensions in QCD. Continuum analyses predict that the difference between $Q^2 F_{\pi}(Q^2)$ and $Q^2 F_{\pi}^M(Q^2)$ becomes noticeable on $Q^2 \gtrsim 5 \text{ GeV}^2$ [57]. However, the difference is only visible because Q^2 becomes large.

If one does not multiply by Q^2 , then, quantitatively, $F_{\pi}^M(Q^2)$ is a fair representation of $F_{\pi}(Q^2)$ on the entire domain of spacelike momenta because the difference between these functions vanishes as $1/Q^2$. We will thus proceed by assuming that $F_{\pi}^M(Q^2)$ is a practicable approximation to $F_{\pi}(Q^2)$, and use the following fact [61]:

$$F_{\pi}^M(Q^2) = (1/2)B(1, 1/2 + Q^2/[2m_M^2]), \quad (9)$$

where the Euler β -function is defined thus:

$$B(1+a, 1+b) = \int_0^1 dy (1-y)^a y^b. \quad (10)$$

In QCD, Eq. (9) and its corollaries (to be explored below) receive small modifications at large Q^2 and, consequently, on the endpoint domains $x \simeq 0, 1$.

The pion form factor can also be expressed in terms of the pion hadron-scale valence quark GPD [54]:

$$F_{\pi}(Q^2) = \int_0^1 dx H^{u\pi}(x, Q^2; \zeta_{\mathcal{H}}), \quad (11)$$

where we have used G -parity symmetry.

The similarity between Eqs. (9), (10) and (11) means that, by exploiting properties of integrable, non-negative and continuously differentiable (C^1) functions on $x \in [0, 1]$, it is readily shown that there is a class of Q^2 -independent C^1 functions, $\{w(x)\}$, satisfying

$$w(0) = 0, \quad w(1) = 1, \quad w'(x) \geq 0, \quad (12)$$

in terms of which one may write [62]

$$H^{u\pi}(x, Q^2; \zeta_{\mathcal{H}}) = \tilde{u}_{\pi}(x; \zeta_{\mathcal{H}})[w(x)]^{Q^2/2m_M^2}, \quad (13a)$$

$$\tilde{u}_{\pi}(x; \zeta_{\mathcal{H}}) = \frac{1}{2}[w(x)]^{-1/2}w'(x) =: a'(x). \quad (13b)$$

Now applying the forward-limit GPD constraint in Eq. (5), one selects a unique member of the class, *i.e.*, the function $w(x)$ for which

$$u_{\pi}(x; \zeta_{\mathcal{H}}) = \tilde{u}_{\pi}(x; \zeta_{\mathcal{H}}) = a'(x) \quad (14)$$

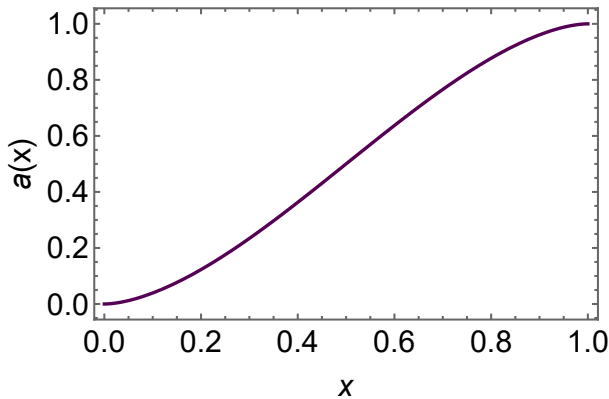


FIG. 1. Solution of Eq. (20), which satisfies the requirements imposed by Eq. (12).

and thereby arrives at a minimal expression for $H^{u\pi}(x, Q^2; \zeta_{\mathcal{H}})$ that complies with Eqs. (5), (11).

We stress that Eq. (14) is valid for any bound state whose electromagnetic form factor is well approximated by a monopole, irrespective of the m_M -value.

4. *Symmetry and the pion $\zeta_{\mathcal{H}}$ valence quark GPD*—The preceding analysis has established that:

$$H^{u\pi}(x, Q^2; \zeta_{\mathcal{H}}) = u_{\pi}(x; \zeta_{\mathcal{H}})[a(x)]^{Q^2/m_M^2}, \quad (15)$$

where $a(x)$ determines and is determined by the pion hadron scale valence quark DF; see Eq. (14). Plainly, therefore, $0 < a(x) < 1$ on $x \in (0, 1)$; hence, with increasing Q^2 , the second factor in Eq. (15) provides damping of the GPD at all x , the rate of which is determined by m_M . The rate decreases as m_M increases; so, more pointlike bound states are associated with Q^2 -flatter GPDs.

Defining $m(x) = (1/m_M^2) \ln[1/a(x)]$, it can be useful to work with the following form of Eq. (15) [63]:

$$H^{u\pi}(x, Q^2; \zeta_{\mathcal{H}}) = u_{\pi}(x; \zeta_{\mathcal{H}}) \exp[-Q^2 m(x)]. \quad (16)$$

For instance, one may now readily obtain

$$|\psi(x, b_{\perp}; \zeta_{\mathcal{H}})|^2 = \frac{u_{\pi}(x; \zeta_{\mathcal{H}})}{4\pi m(x)} \times (1-x)^2 \exp\left[-\frac{(1-x)^2 b_{\perp}^2}{4m(x)}\right]. \quad (17)$$

From this expression, the distribution amplitude (DA) associated with the pion's two dressed valence parton component is directly obtain via

$$\varphi_{\pi}(x; \zeta_{\mathcal{H}}) = 2\pi |\psi(x, b_{\perp} = 0; \zeta_{\mathcal{H}})|/m_M \quad (18a)$$

$$= (1-x)(\pi u_{\pi}(x; \zeta_{\mathcal{H}})/\ln[1/a(x)])^{\frac{1}{2}}. \quad (18b)$$

Now, using Eq. (12), the DF symmetry property, Eq. (2), entails

$$a(x) + a(1-x) = 1. \quad (19)$$

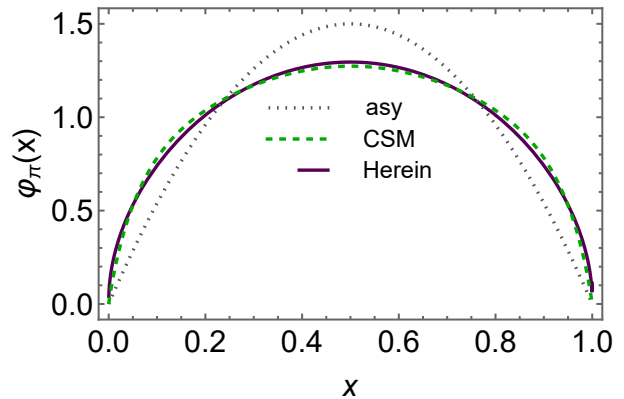


FIG. 2. Pion valence quark DA, Eq. (18). Legend: solid purple curve – result obtained herein using $a(x)$ from Fig. 1 and Eq. (14); dashed green curve – CSM prediction [40, 64]; dotted grey curve – asymptotic twist-two pion DA [58–60].

Subsequently using the GPD symmetry property, Eq. (7), one arrives at the following “master equation”:

$$1 - a(x) = [a(x)]^{x^2/(1-x)^2}. \quad (20)$$

It is worth reiterating that this identity is valid for any bound state whose electromagnetic form factor is well approximated by a monopole, irrespective of the m_M -value. No other dynamical information is required to fix the form of $a(x)$ and, hence, the pion hadron scale valence quark GPD.

5. *Distribution amplitudes and functions*—The solution of Eq. (20) is drawn in Fig. 1. For practical applications, it is well approximated by the following polynomial:

$$a(x) \approx 0.195x + 2.415x^2 - 1.610x^3. \quad (21)$$

Nevertheless, herein, we employ the numerically obtained result; and, for future use, note that the true large- x behaviour is as follows:

$$a(x) \stackrel{x \simeq 1}{\simeq} 1 - 1.581(1-x)^2 \ln 1/(1-x) - 5.458(1-x)^4 [\ln 1/(1-x)]^2 + \dots, \quad (22)$$

with the profile on $x \simeq 0$ obtained via Eq. (19).

Using the solution of Eq. (20), one obtains the pion valence quark DA drawn in Fig. 2. It has the following endpoint behaviour, obtained with Eqs. (14), (18), (22):

$$\varphi_{\pi}(x) \stackrel{x \simeq 1}{\simeq} 2.507\sqrt{1-x} + \dots \quad (23)$$

The $x \simeq 0$ form is given by $x \leftrightarrow (1-x)$ symmetry; and $\int_0^1 dx (2x-1)^2 \varphi_{\pi}(x) = 0.246 =: \langle \xi^2 \rangle_{\varphi_{\pi}}$.

The solution is compared in Fig. 2 with the continuum Schwinger function method (CSM) prediction [40, 64], obtained using a Bethe-Salpeter kernel for the pion bound state equation which maintains a rigorous link with pQCD and, consequently, ensures that scaling violations are expressed in the pion elastic electromagnetic

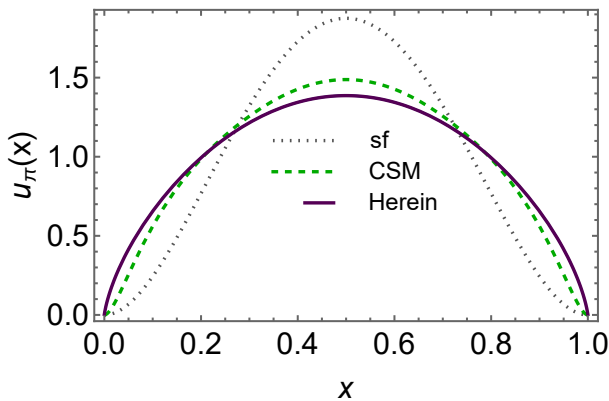


FIG. 3. Pion valence quark DF. Legend: solid purple curve – result obtained herein using $a(x)$ from Fig. 1 and Eq. (14); dashed green curve – CSM prediction [40, 65]; dotted grey curve – scale free DF (see text).

form factor; see also Ref. [57]. The CSM DA prediction is almost indistinguishable from the symmetry-driven result obtained herein, *e.g.*, $\langle \xi^2 \rangle_{\varphi_{\pi}^{\text{CSM}}} = 0.247$. Those small differences which do exist are merely an expression of the absence of scaling violations in the monopole approximation to $F_{\pi}(Q^2)$, Eq. (9). (One may verify this by changing the monopole power from $1 \rightarrow 1 + \epsilon$, with $\epsilon \simeq 0$ serving to mockup a \ln -correction.) This is also reflected in a different endpoint behaviour: $\varphi_{\pi}^{\text{CSM}} \approx 20.28(1-x)$ on $x \simeq 1$, again with the $x \simeq 0$ result given by $x \leftrightarrow (1-x)$ symmetry, and again with endpoint power-law behaviour that is consistent with QCD expectations. The remaining curve in Fig. 2 is the pQCD prediction for the asymptotic twist-two pion DA, valid for ζ in the neighbourhood $\zeta_{\mathcal{H}}/\zeta \simeq 0$: $\varphi_{\text{asy}} = 6x(1-x)$, $\langle \xi^2 \rangle_{\varphi_{\text{asy}}} = 0.2$.

Plainly, the symmetry properties discussed in Sec. 2 entail that, for any meson whose electromagnetic form is well approximated by a monopole, the DA associated with the two dressed valence parton component is a dilated, concave function, much broader and flatter than the asymptotic DA. This is a model-independent result.

With the information now in hand, one readily arrives at the hadron scale DF depicted in Fig. 3. The endpoint behaviour of this $x \leftrightarrow (1-x)$ symmetric function is:

$$u_{\pi}(x) \stackrel{x \simeq 1}{\approx} 3.163(1-x) \ln 1/(1-x) + \dots \quad (24)$$

Once again, the image compares the symmetry-based result with the CSM prediction [40, 65]. In this case, too, there is qualitative and semi-quantitative agreement; and, once more, the differences owe to the omission of scaling violations in the monopole approximation to the pion elastic electromagnetic form factor, which are also expressed in a different endpoint behaviour: $u_{\pi}^{\text{CSM}}(x) \approx 375.3(1-x)^2$ on $x \simeq 1$. Owing to its connection with QCD, the CSM prediction expresses the power law behaviour predicted by strong interaction theory [18, 66–69]. The other curve in Fig. 3 is the scale-free DF: $q_{\text{sf}} = 30x^2(1-x)^2$, which is a DF analogue of φ_{asy} .

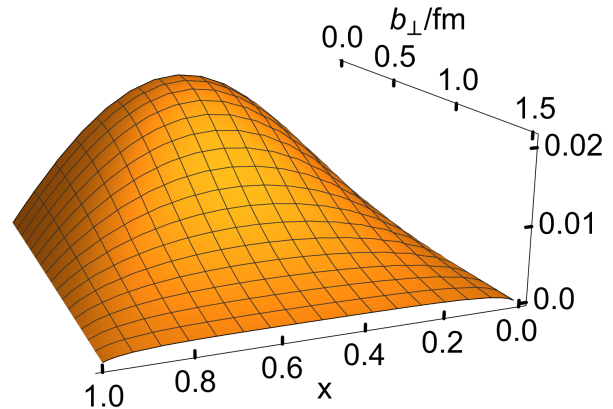


FIG. 4. Hadron scale valence quark symmetrised-GPD in impact parameter space, Eqs. (3), (17).

Evidently, the symmetry properties discussed in Sec. 2 ensure that, for any meson whose elastic electromagnetic form is well approximated by a monopole, the hadron scale valence quark DF is a dilated function. Again, this is a model-independent result.

Before providing a comparison with experiment, it is worth displaying the $\zeta_{\mathcal{H}}$ valence-quark symmetrised-GPD in impact-parameter space, Eqs. (3), (17); see Fig. 4. Naturally, the result is symmetric under $x \leftrightarrow (1-x)$. Moreover, owing to the absence of scaling violations in the monopole approximation to the electromagnetic form factor, then, at fixed- x , the b_{\perp} profile is Gaussian with magnitude and range characterised by m_M .

6. Validation by experiment — As noted in the Introduction, data relating to the pion valence quark DF are available [14, 15, E615]. Their interpretation remains controversial, with different phenomenological analysis methods yielding conflicting results [18]. The existing data are from $\pi + W$ Drell-Yan reactions performed more than thirty-five years ago, at an average centre-of-mass energy $\zeta_5 = 5.2 \text{ GeV}$. Relevant new data are expected to be obtained by the AMBER Collaboration [70, 71] and, potentially, via experiments at Jefferson Laboratory [72] or an electron ion collider [73, 74]. Meanwhile, comparisons can only be made with E615 data.

In connecting $\zeta_{\mathcal{H}} \rightarrow \zeta_5$, we use the AO scheme [36] for evolving the results in Fig. 3. To implement this, one only requires knowledge of the light-front momentum fraction carried by valence quarks at ζ_5 , since the hadron scale value is one-half by definition. A unifying analysis of results obtained using continuum and lattice Schwinger function methods yields $\langle x \rangle_{u_{\pi}}^{\zeta_5} = 0.21(1)$ [69]. Working with this information, the AO procedure delivers the solid purple curve in Fig. 5. The associated bracketing band expresses the $\approx 5\%$ uncertainty in the momentum fraction. On $x \gtrsim 0.85$, the symmetry-based results are well described by a simple power-law: $c(1-x)^{\beta}$, $\beta = 1.99 \pm 0.06$, $c = 1.88 \mp 0.09$. Similarly, the dashed green curve and band represent AO evolution of the CSM prediction: on $x \gtrsim 0.85$, they can be described

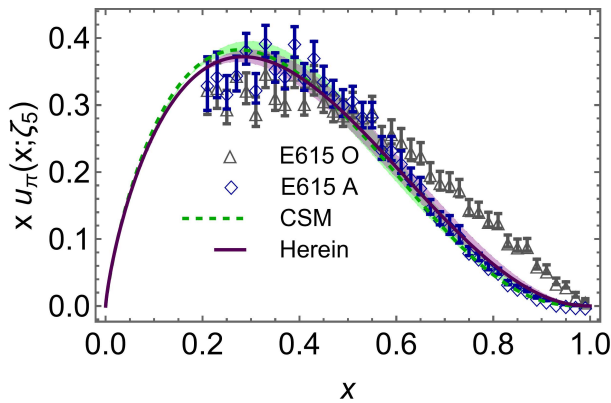


FIG. 5. Pion valence quark DF at the scale, $\zeta_5 = 5.2$ GeV. Legend: solid purple curve and band – symmetry-driven result obtained herein, Eq. (14); dashed green curve and band – CSM prediction [40, 65]; open blue diamonds – E615 data analysed as described in Refs. [75, 76], with soft-gluon resummation; open grey up-triangles – data inferred via leading-order analysis of the Drell-Yan cross section [14]

by $c(1-x)^\beta$, $\beta = 2.79 \pm 0.08$, $c = 7.54 \mp 0.07$. Evidently, since the differences are small, it is unlikely that any foreseeable experiment could achieve sufficient precision to enable analysis thereof to distinguish between the symmetry-based result obtained herein and the re-

alistic CSM prediction; hence, for all intents and purposes, they are equivalent. Importantly, both predictions unambiguously favour the analysis of E615 data described in Refs. [75, 76], which includes soft gluon resummation and, like the symmetry-based and CSM predictions, yields large- x behaviour that is practically consistent with pQCD expectations [18, 66–69].

7. Conclusion — Unveiling the structure of Nature’s most fundamental Nambu-Goldstone boson – the pion – is a high-priority goal of modern hadroparticle physics. Using the theory of effective charges in QCD and the fact that the Q^2 -dependence of the charged-pion elastic electromagnetic form factor is well approximated by a monopole, we delivered a model-independent, parameter-free prediction for the pion’s valence-quark momentum-fraction probability distribution function [Fig. 5]. Crucially, its behaviour on the valence domain of light-front momentum fraction is practically consistent with QCD expectations. Our result confirms those obtained using continuum and lattice Schwinger function methods [18, 69]; hence may serve as additional motivation for future experiments that aim to resolve existing pion DF controversies [70–74, 77].

Acknowledgments — Work supported by: National Natural Science Foundation of China, grant no. 12135007; and Spanish Ministry of Science and Innovation (MICINN) grant no. PID2022-140440NB-C22).

-
- [1] S. Navas, et al., Review of particle physics, Phys. Rev. D 110 (3) (2024) 030001.
- [2] J. E. Lynn, I. Tews, S. Gandolfi, A. Lovato, Quantum Monte Carlo Methods in Nuclear Physics: Recent Advances, Ann. Rev. Nucl. Part. Sci. 69 (2019) 279–305.
- [3] K. D. Launey, A. Mercenne, T. Dytrych, Nuclear Dynamics and Reactions in the Ab Initio Symmetry-Adapted Framework, Ann. Rev. Nucl. Part. Sci. 71 (2021) 253–277.
- [4] B. Ananthanarayan, M. S. A. A. Khan, D. Wyler, Chiral perturbation theory: reflections on effective theories of the standard model, Indian J. Phys. 97 (11) (2023) 3245–3267.
- [5] H. Fritzsch, M. Gell-Mann, H. Leutwyler, Advantages of the Color Octet Gluon Picture, Phys. Lett. B 47 (1973) 365–368.
- [6] K. D. Lane, Asymptotic Freedom and Goldstone Realization of Chiral Symmetry, Phys. Rev. D 10 (1974) 2605.
- [7] P. Maris, C. D. Roberts, π and K meson Bethe-Salpeter amplitudes, Phys. Rev. C 56 (1997) 3369–3383.
- [8] F. J. Llanes-Estrada, S. R. Cotanch, Relativistic many body Hamiltonian approach to mesons, Nucl. Phys. A 697 (2002) 303–337.
- [9] P. Bicudo, S. Cotanch, F. J. Llanes-Estrada, P. Maris, E. Ribeiro, A. Szczepaniak, Chirally symmetric quark description of low energy $\pi\pi$ scattering, Phys. Rev. D 65 (2002) 076008.
- [10] S.-X. Qin, C. D. Roberts, S. M. Schmidt, Ward-Green-Takahashi identities and the axial-vector vertex, Phys. Lett. B 733 (2014) 202–208.
- [11] E. B. Dally, et al., Elastic Scattering Measurement of the Negative Pion Radius, Phys. Rev. Lett. 48 (1982) 375–378.
- [12] S. R. Amendolia, et al., A Measurement of the Pion Charge Radius, Phys. Lett. B 146 (1984) 116.
- [13] S. R. Amendolia, et al., A Measurement of the Space-Like Pion Electromagnetic Form-Factor, Nucl. Phys. B 277 (1986) 168.
- [14] J. S. Conway, et al., Experimental study of muon pairs produced by 252-GeV pions on tungsten, Phys. Rev. D 39 (1989) 92–122.
- [15] K. Wijesooriya, P. E. Reimer, R. J. Holt, The pion parton distribution function in the valence region, Phys. Rev. C 72 (2005) 065203.
- [16] M. Derrick, et al., Observation of events with an energetic forward neutron in deep inelastic scattering at HERA, Phys. Lett. B 384 (1996) 388–400.
- [17] C. Adloff, et al., Measurement of leading proton and neutron production in deep inelastic scattering at HERA, Eur. Phys. J. C 6 (1999) 587–602.
- [18] Z. F. Cui, M. Ding, J. M. Morgado, K. Raya, D. Binosi, L. Chang, J. Papavassiliou, C. D. Roberts, J. Rodríguez-Quintero, S. M. Schmidt, Concerning pion parton distributions, Eur. Phys. J. A 58 (1) (2022) 10.
- [19] W. de Paula, E. Ydrefors, J. H. Nogueira Alvarenga, T. Frederico, G. Salmè, Parton distribution function in a pion with Minkowskian dynamics, Phys. Rev. D 105 (7) (2022) L071505.

- [20] M. Ahmady, S. Kaur, C. Mondal, R. Sandapen, Pion spectroscopy and dynamics using the holographic light-front Schrödinger equation and the 't Hooft equation, *Phys. Lett. B* 836 (2023) 137628.
- [21] W.-C. Chang, J.-C. Peng, S. Platchkov, T. Sawada, Fixed-target charmonium production and pion parton distributions, *Phys. Rev. D* 107 (5) (2023) 056008.
- [22] B. Pasquini, S. Rodini, S. Venturini, Valence quark, sea, and gluon content of the pion from the parton distribution functions and the electromagnetic form factor, *Phys. Rev. D* 107 (11) (2023) 114023.
- [23] M. Alberg, G. A. Miller, Quark counting, Drell-Yan West, and the pion wave function, *Phys. Rev. C* 110 (4) (2024) L042201.
- [24] H.-M. Choi, C.-R. Ji, Consistency of the pion form factor and unpolarized transverse momentum dependent parton distributions beyond leading twist in the light-front quark model, *Phys. Rev. D* 110 (1) (2024) 014006.
- [25] J. Lan, C. Mondal, X. Zhao, T. Frederico, J. P. Vary, Gluonic contributions to the pion parton distribution functions, *Phys. Rev. D* 111 (11) (2025) L111903.
- [26] H.-W. Lin, Mapping parton distributions of hadrons with lattice QCD, *Prog. Part. Nucl. Phys.* 144 (2025) 104177.
- [27] G. Grunberg, Renormalization Group Improved Perturbative QCD, *Phys. Lett. B* 95 (1980) 70, [Erratum: *Phys. Lett. B* 110, 501 (1982)].
- [28] G. Grunberg, Renormalization Scheme Independent QCD and QED: The Method of Effective Charges, *Phys. Rev. D* 29 (1984) 2315.
- [29] A. Deur, S. J. Brodsky, C. D. Roberts, QCD Running Couplings and Effective Charges, *Prog. Part. Nucl. Phys.* 134 (2024) 104081.
- [30] A. Deur, V. Burkert, J. P. Chen, W. Korsch, Experimental determination of the QCD effective charge $\alpha_{g_1}(Q)$, *Particles* 5 (2) (2022) 171–179.
- [31] M. Gell-Mann, F. E. Low, Quantum electrodynamics at small distances, *Phys. Rev.* 95 (1954) 1300–1312.
- [32] Y. L. Dokshitzer, Calculation of the Structure Functions for Deep Inelastic Scattering and $e^+ e^-$ Annihilation by Perturbation Theory in Quantum Chromodynamics. (In Russian), *Sov. Phys. JETP* 46 (1977) 641–653.
- [33] V. N. Gribov, L. N. Lipatov, Deep inelastic electron scattering in perturbation theory, *Phys. Lett. B* 37 (1971) 78–80.
- [34] L. N. Lipatov, The parton model and perturbation theory, *Sov. J. Nucl. Phys.* 20 (1975) 94–102.
- [35] G. Altarelli, G. Parisi, Asymptotic Freedom in Parton Language, *Nucl. Phys. B* 126 (1977) 298–318.
- [36] P.-L. Yin, Y.-Z. Xu, Z.-F. Cui, C. D. Roberts, J. Rodríguez-Quintero, All-Orders Evolution of Parton Distributions: Principle, Practice, and Predictions, *Chin. Phys. Lett. Express* 40 (9) (2023) 091201.
- [37] T. D. Lee, C.-N. Yang, Charge Conjugation, a New Quantum Number G , and Selection Rules Concerning a Nucleon Anti-nucleon System, *Nuovo Cim.* 10 (1956) 749–753.
- [38] M. B. Hecht, C. D. Roberts, S. M. Schmidt, Valence-quark distributions in the pion, *Phys. Rev. C* 63 (2001) 025213.
- [39] Z. Q. Yao, Y. Z. Xu, D. Binosi, Z. F. Cui, M. Ding, K. Raya, C. D. Roberts, J. Rodríguez-Quintero, Pion, Kaon and nucleon gravitational form factors – arXiv:2503.23166 [hep-ph], in: *Proceedings of the 16th Conference on Quark Confinement and the Hadron Spectrum*, 2025.
- [40] Z.-F. Cui, M. Ding, F. Gao, K. Raya, D. Binosi, L. Chang, C. D. Roberts, J. Rodríguez-Quintero, S. M. Schmidt, Kaon and pion parton distributions, *Eur. Phys. J. C* 80 (2020) 1064.
- [41] L. Chang, F. Gao, C. D. Roberts, Parton distributions of light quarks and antiquarks in the proton, *Phys. Lett. B* 829 (2022) 137078.
- [42] Y. Lu, L. Chang, K. Raya, C. D. Roberts, J. Rodríguez-Quintero, Proton and pion distribution functions in counterpoint, *Phys. Lett. B* 830 (2022) 137130.
- [43] P. Cheng, Y. Yu, H.-Y. Xing, C. Chen, Z.-F. Cui, C. D. Roberts, Perspective on polarised parton distribution functions and proton spin, *Phys. Lett. B* 844 (2023) 138074.
- [44] Y. Yu, P. Cheng, H.-Y. Xing, F. Gao, C. D. Roberts, Contact interaction study of proton parton distributions, *Eur. Phys. J. C* 84 (7) (2024) 739.
- [45] Y. Yu, P. Cheng, H.-Y. Xing, D. Binosi, C. D. Roberts, Distribution Functions of Λ and Σ^0 Baryons, *Eur. Phys. J. A* 61 (9) (2025) 208.
- [46] Y.-Z. Xu, K. Raya, Z.-F. Cui, C. D. Roberts, J. Rodríguez-Quintero, Empirical Determination of the Pion Mass Distribution, *Chin. Phys. Lett. Express* 40 (4) (2023) 041201.
- [47] Z.-N. Xu, D. Binosi, C. Chen, K. Raya, C. D. Roberts, J. Rodríguez-Quintero, Kaon distribution functions from empirical information, *Phys. Lett. B* 865 (2025) 139451.
- [48] Y. Yu, C. D. Roberts, Impressions of Parton Distribution Functions, *Chin. Phys. Lett.* 41 (2024) 121202.
- [49] H.-Y. Xing, W.-H. Bian, Z.-F. Cui, C. D. Roberts, Kaon and Pion Fragmentation Functions – arXiv:2504.08142 [hep-ph].
- [50] Z. Q. Yao, Y. Z. Xu, D. Binosi, Z. F. Cui, M. Ding, K. Raya, C. D. Roberts, J. Rodríguez-Quintero, S. M. Schmidt, Nucleon gravitational form factors, *Eur. Phys. J. A* 61 (5) (2025) 92.
- [51] D. Binosi, C. D. Roberts, Z.-Q. Yao, Hadron Structure: Perspective and Insights. arXiv:2503.05984 [hep-ph], in: 16th Conference on Quark Confinement and the Hadron Spectrum, 2025.
- [52] M. Diehl, T. Feldmann, R. Jakob, P. Kroll, The Overlap representation of skewed quark and gluon distributions, *Nucl. Phys. B* 596 (2001) 33–65.
- [53] M. Burkardt, Impact parameter space interpretation for generalized parton distributions, *Int. J. Mod. Phys. A* 18 (2003) 173–208.
- [54] M. Diehl, Generalized parton distributions, *Phys. Rept.* 388 (2003) 41–277.
- [55] T. Horn, et al., Scaling study of the pion electroproduction cross sections and the pion form factor, *Phys. Rev. C* 78 (2008) 058201.
- [56] G. Huber, et al., Charged pion form-factor between $Q^2 = 0.60 \text{ GeV}^2$ and 2.45 GeV^2 . II. Determination of, and results for, the pion form-factor, *Phys. Rev. C* 78 (2008) 045203.
- [57] Z.-Q. Yao, D. Binosi, C. D. Roberts, Onset of scaling violation in pion and kaon elastic electromagnetic form factors, *Phys. Lett. B* 855 (2024) 138823.
- [58] G. P. Lepage, S. J. Brodsky, Exclusive Processes in Quantum Chromodynamics: Evolution Equations for Hadronic Wave Functions and the Form-Factors of Mesons, *Phys. Lett. B* 87 (1979) 359–365.
- [59] A. V. Efremov, A. V. Radyushkin, Factorization and

- Asymptotical Behavior of Pion Form-Factor in QCD, *Phys. Lett. B* 94 (1980) 245–250.
- [60] G. P. Lepage, S. J. Brodsky, Exclusive Processes in Perturbative Quantum Chromodynamics, *Phys. Rev. D* 22 (1980) 2157–2198.
- [61] L. Chang, K. Raya, X. Wang, Pion Parton Distribution Function in Light-Front Holographic QCD, *Chin. Phys. C* 44 (11) (2020) 114105.
- [62] X. Wang, Z. Xing, L. Chang, M. Ding, K. Raya, C. D. Roberts, Sketching pion and proton mass distributions, *Phys. Lett. B* 862 (2025) 139280.
- [63] K. Raya, A. Bashir, J. Rodríguez-Quintero, Mapping Spatial Distributions within Pseudoscalar Mesons, *Chin. Phys. Lett.* 42 (2) (2025) 020201.
- [64] L. Chang, I. C. Cloet, J. J. Cobos-Martinez, C. D. Roberts, S. M. Schmidt, P. C. Tandy, Imaging dynamical chiral symmetry breaking: pion wave function on the light front, *Phys. Rev. Lett.* 110 (2013) 132001.
- [65] M. Ding, K. Raya, D. Binosi, L. Chang, C. D. Roberts, S. M. Schmidt, Symmetry, symmetry breaking, and pion parton distributions, *Phys. Rev. D* 101 (5) (2020) 054014.
- [66] S. J. Brodsky, M. Burkardt, I. Schmidt, Perturbative QCD constraints on the shape of polarized quark and gluon distributions, *Nucl. Phys. B* 441 (1995) 197–214.
- [67] F. Yuan, Generalized parton distributions at $x \rightarrow 1$, *Phys. Rev. D* 69 (2004) 051501.
- [68] R. J. Holt, C. D. Roberts, Distribution Functions of the Nucleon and Pion in the Valence Region, *Rev. Mod. Phys.* 82 (2010) 2991–3044.
- [69] Y. Lu, Y.-Z. Xu, K. Raya, C. D. Roberts, J. Rodríguez-Quintero, Pion distribution functions from low-order Mellin moments, *Phys. Lett. B* 850 (2024) 138534.
- [70] C. Quintans, The New AMBER Experiment at the CERN SPS, *Few Body Syst.* 63 (4) (2022) 72.
- [71] B. Seitz, AMBER: a new QCD facility at the CERN SPS M2 beam line, *PoS ICHEP2022* (2023) 839.
- [72] T. Horn, C. D. Roberts, The pion: an enigma within the Standard Model, *J. Phys. G* 43 (2016) 073001.
- [73] X. Chen, F.-K. Guo, C. D. Roberts, R. Wang, Selected Science Opportunities for the EicC, *Few Body Syst.* 61 (2020) 43.
- [74] J. Arrington, et al., Revealing the structure of light pseudoscalar mesons at the electron-ion collider, *J. Phys. G* 48 (2021) 075106.
- [75] M. Aicher, A. Schäfer, W. Vogelsang, Soft-Gluon Resummation and the Valence Parton Distribution Function of the Pion, *Phys. Rev. Lett.* 105 (2010) 252003.
- [76] L. Chang, C. Mezrag, H. Moutarde, C. D. Roberts, J. Rodríguez-Quintero, P. C. Tandy, Basic features of the pion valence-quark distribution function, *Phys. Lett. B* 737 (2014) 23–29.
- [77] C. D. Roberts, D. G. Richards, T. Horn, L. Chang, Insights into the emergence of mass from studies of pion and kaon structure, *Prog. Part. Nucl. Phys.* 120 (2021) 103883.